Nussbaum, J. L., & Roussel, G. (1983) *Cell. Tissue Res. 234*, 547–559.
Papahadjopoulos, D., Vail, W. J., & Moscarello, M. A. (1975) *J. Membr. Biol. 22*, 143–164.
Phillips, P. C., Williams, R. M., & Chapman, D. (1969) *Chem. Phys. Lipids 3*, 234–244.
Pottel, H., Van der Meer, W., & Herreman, W. (1983) *Biochim. Biophys. Acta 730*, 181–186.
Rice, D. M., Meadow, M. D., Scheiman, A. O., Goni, F. M., Gomez-Fernandez, J. C., Moscarello, M. A., Chapman, D., & Oldfield, E. (1979) *Biochemistry 18*, 5893–5903.
Schlesinger, M. J. (1981) *Annu. Rev. Biochem. 50*, 193–206.
Sherman, G., & Folch-Pi, J. (1970) *J. Neurochem. 17*, 597–605.
Silvius, J. R., Birell, G. B., Boggs, J. M., Jost, P. C., & Griffith, O. H. (1983) *Biophys. J. 41*, 243–246.
Stoffel, W., Shröder, W., Hiller, H., & Deutzman, R. (1984) *Hoppe Seyler's Z. Physiol. Chem. 364*, 1455–1466.
Stoffyn, P., & Folch-pi, J. (1971) *Biochem. Biophys. Res. Commun. 44*, 157–161.
Suukuursk, J., Lentz, B. R., Barenholz, Y., Biltonen, R., & Thompson, T. E. (1976) *Biochemistry 15*, 1393–1401.
Szuchet, S., Yim, S. H., & Monsma, S. (1983) *Proc. Natl. Acad. Sci. U.S.A. 80*, 7019–7023.
Tennebaum, D., & Folch-Pi, J. (1966) *Biochim. Biophys. Acta 115*, 141–143.
Ting-Beall, H. P., Lees, M. B., & Robertson, J. D. (1979) *J. Membr. Biol. 51*, 33–46.
Vacher, M., Waks, M., & Nicot, C. (1984) *Biochem. J. 218*, 197–202.
Van Blitterswijk, W. J., Van Hoeven, R. P., & Van der Meer, B. W. (1981) *Biochim. Biophys. Acta 644*, 323–332.

Advantages and Limitations of 1-Palmitoyl-2-[[2-[4-(6-phenyl-*trans*-1,3,5-hexatrienyl)phenyl]ethyl]carbonyl]-3-*sn*-phosphatidylcholine as a Fluorescent Membrane Probe†

Roberta A. Parente and Barry R. Lentz*
Department of Biochemistry and Nutrition, University of North Carolina, Chapel Hill, North Carolina 27514
Received January 3, 1985

ABSTRACT: We have investigated the behavior of 1-palmitoyl-2-[[2-[4-(6-phenyl-*trans*-1,3,5-hexatrienyl)phenyl]ethyl]carbonyl]-3-*sn*-phosphatidylcholine (DPHpPC) in synthetic, multilamellar phosphatidylcholine vesicles. This fluorescent phospholipid has photophysical properties similar to its parent fluorophore, diphenylhexatriene (DPH). DPHpPC preferentially partitioned into fluid phase lipid ($K_{f/s}$ = 3.3) and reported a lower phase transition temperature as detected by fluorescence anisotropy than that observed by differential scanning calorimetry. Calorimetric measurements of the bilayer phase transition in samples having different phospholipid to probe ratios demonstrated very slight changes in membrane phase transition temperature (0.1–0.2 °C) and showed no measurable change in transition width. Nonetheless, measurements of probe fluorescence properties suggested that DPHpPC disrupts its local environment in the membrane and may even induce perturbed probe-rich local domains below the phospholipid phase transition. Temperature profiles of steady-state fluorescence anisotropy, limiting anisotropy, differential tangent, and rotational rate were similar to those of DPH below the main lipid phase transition but indicated more restricted rotational motion above the lipid phase transition temperature. As for DPH, the fluorescence decay of DPHpPC could be described by either a single or double exponential both above and below the DPPC phase transition. The choice seemed dependent on the treatment of the sample. The intensity-weighted average lifetime of DPHpPC was roughly 1.5 ns shorter than that of DPH. In summary, the measured properties of DPHpPC and its lipid-like structure make it a powerful probe of membrane structure and dynamics.

For years, fluorescent probes have provided insight into the structure and dynamics of biomembranes. The ideal probe (1) is sensitive to the motions of individual molecules on the nanosecond timescale of fluorescence measurements, (2) has a high extinction coefficient and quantum yield, (3) has broad absorption and emission limits, (4) does little to interfere with the natural packing arrangement of the bilayer, and (5) has a fixed orientation in the bilayer. These characteristics enable the user to (1) obtain high fluorescence intensity with minimal use of probe, (2) to work over a wide range of wavelengths, (3) to avoid measuring artifacts in bilayer behavior induced by bulky probe molecules, and (4) to define the environment surrounding the probe.

Diphenylhexatriene (DPH)[1] has many attributes of an ideal probe and has been successfully used to study lipid bilayer

† This work was supported by NIH Grant GM32707.

[1] Abbreviations: DMPC, 1,2-dimyristoyl-3-*sn*-phosphatidylcholine; DPPC, 1,2-dipalmitoyl-3-*sn*-phosphatidylcholine; DSPC, 1,2-distearoyl-3-*sn*-phosphatidylcholine; DPHpPC, 1-palmitoyl-2-[[2-[4-(6-phenyl-*trans*-1,3,5-hexatrienyl)phenyl]ethyl]carbonyl]-3-*sn*-phosphatidylcholine; DPH, 1,6-diphenyl-*trans*-1,3,5-hexatriene; TMA-DPH, 1-[4-(trimethylammonio)phenyl]-6-phenyl-1,3,5-hexatriene; DPHePC, phosphatidylcholine derived from egg yolk lysophosphatidylcholine with propionyl-DPH esterified to the 2-position of glycerol; POPOP, 2,2′-(*p*-phenylene)bis(5-phenyloxazole); LMV, large, multilamellar vesicle(s).

0006-2960/85/0424-6178$01.50/0

structure over the past several years (Shinitzky & Barenholz, 1978). DPH is readily soluble in the hydrocarbon chain region of lipid bilayers. However, the uncertain orientation of DPH within the membrane has drawn criticism, especially when the probe has greater motional freedom (i.e., above the lipid phase transition). Recently, several DPH analogues have been synthesized in which the fluorophore's location in the bilayer can be better estimated (Prendergast et al., 1981; Morgan et al., 1982; Cranny et al., 1983). In one such analogue, 1-[4-(trimethylammonio)phenyl]-6-phenyl-1,3,5-hexatriene (TMA-DPH),[1] the DPH moiety is thought to reside in the lipid hydrocarbon region while the cationic trimethylamino head group is likely positioned at the lipid–water interface (Prendergast et al., 1981). This probe, like its parent molecule, is able to exchange freely through solution and redistribute into unlabeled phospholipid dispersions (R. A. Parente and B. R. Lentz, unpublished results).

Another analogue, 1-palmitoyl-2-[[2-[4-(6-phenyl-*trans*-1,3,5-hexatrienyl)phenyl]ethyl]carbonyl]-3-*sn*-phosphatidylcholine (DPHpPC),[1] incorporates the DPH moiety into a phospholipid at the 2-position, replacing a normal hydrocarbon chain. As with TMA-DPH, the fluorophore portion of this molecule is oriented perpendicular to the bilayer plane. In addition, DPHpPC would not be expected to undergo rapid exchange between membranes (Morgan et al., 1982), making it beneficial for monitoring vesicle fusion. Finally, being a lipid-like molecule, this probe should not significantly perturb bilayer packing and should display motional properties that reflect the behavior of neighboring bilayer components. Unfortunately, limited data exist to establish the motional and perturbing properties of DPHpPC. In this paper, we report the partitioning properties of DPHpPC, determine its ability to detect a lipid phase transition, monitor its lifetime behavior, ascertain its motional parameters in phospholipid dispersions, and determine the extent to which it perturbs membrane structure. These observations are used to establish the usefulness of DPHpPC as a probe of bilayer structure and dynamics.

Materials and Methods

Materials

Chloroform stocks of 1,2-dipalmitoyl-3-*sn*-phosphatidylcholine (DPPC),[1] 1,2-dimyristoyl-3-*sn*-phosphatidylcholine (DMPC),[1] and 1,2-distearoyl-3-*sn*-phosphatidylcholine (DSPC)[1] were purchased from Avanti Polar Lipids, Inc. (Birmingham, AL). DPPC was filtered once before use over Norit-A neutral activated charcoal to remove fluorescent contamination. All lipids were found to be greater than 99% pure when chromatographed on Analtech GHL plates (impregnated with 0.01 M dipotassium oxalate) developed in $CHCl_3$–CH_2OH–H_2O (65:25:4 v/v/v) and stained with iodine. A small amount (~0.15 mg) of a DPH-containing phosphatidylcholine prepared from egg yolk lysophosphatidylcholine (DPHePC;[1] Morgan et al., 1982) was a generous gift of E. W. Thomas and Y. Yianni (Salford, U.K.). Additional 4-(2-carboxyethyl)-DPH was obtained from E. Thomas (Salford, U.K.) and converted to DPHpPC by Dr. Walter Shaw of Avanti Polar Lipids. TLC plates were run in the solvent system above and visualized by UV light followed by iodine staining. For both DPHpPC and DPHePC, only one spot was seen under UV light; however, in the Thomas preparation, iodine staining revealed a small second spot that migrated near the solvent front, while no second spot was observed in the Avanti preparation. Unless specifically stated, the results obtained with the two preparations were identical. Use of the Thomas preparation of DPHePC enabled us to compare our results with other studies (Cranney et al., 1983; Stubbs et al., 1984) using the egg lipid based preparation. Ultrapure KCl was from Heico, Inc. (Delaware Water Gap, PA; lot 2179). KCl solutions were twice filtered through a 0.22-μm Millipore filter prior to use. Amberized glassware was purchased from Reliance Glass Works, Inc. (Bensenville, IL).

Methods

Vesicle Preparation. Lipid and probe (DPHpPC or DPHePC) stocks were mixed in a ratio of 400:1 (unless otherwise stated) and dried under argon onto the wall of a round-bottom flask. The lipid film was subjected to high vacuum (0.5 mmHg) for 8–12 h to remove any residual solvent. Large, multilamellar vesicles (LMV) were prepared in 50 mM KCl as described previously (Lentz et al., 1976). Samples were stored under argon and swirled at 48 °C in a rotary incubator for at least 2 h prior to use. DPHpPC was found to be fairly sensitive to photolysis. Thus, samples were prepared and stored in amberized glassware or in the dark to prevent light-induced photolysis. No problems were encountered when samples were treated in this manner. The exact mechanism of this light sensitivity was not investigated.

Fluorescence. All fluorescence measurements were made on an SLM 4800 spectrofluorometer (SLM Instruments, Urbana, IL) equipped with a modified, multitemperature cuvette holder (Barrow & Lentz, 1985). Excitation was with the 366-nm mercury line of a 200-W mercury–xenon lamp (Canrad-Hanovia, Newark, NJ). For lifetime data collection, a single polarizer was set at 35° from vertical in the excitation path. Emission was detected with a 3-mm high-pass KV-450 filter (50% transmittance at 450 nm, Schott Optical Glass, Duryea, PA). Lifetime measurements were performed by the phase and modulation method of Spencer & Weber (1969) with modifications described by Barrow & Lentz 1983). DPPC LMV samples (0.25 mM) were examined at modulation frequencies of 6, 18, and 30 MHz. An isochronal standard of DPH in heptane (τ = 6.75 ns; 2×10^{-7} M) was used as a reference for lifetime measurements (Barrow & Lentz, 1983, 1985). The lifetime of the standard was determined at 23 °C against a reference of POPOP in absolute ethanol. The reference standard was maintained at 23 °C, while the temperature in the other two positions of the cuvette holder was variable. The background fluorescence intensity of vesicle samples devoid of probe was measured to be less than 0.5% of the fluorescent samples. Corrections were made for blank intensities when they were above this limit. Fluorescence decays could be routinely resolved in terms of two lifetime components (Barrow & Lentz, 1983, 1985).

Differential tangent measurements were made on a 0.1 mM DPPC LMV sample by the method described by Lakowicz et al. (1979), with the exciting light polarized vertically and sinusoidally modulated at 18 and 30 mHz. Calculations of differential tangents (tan Δ), rotational rate (R), and limiting anisotropy (r_∞) were performed following equations 17 and 18 of Lakowicz et al. (1979). The average lifetime (weighted by the fractional intensity [f] of each component) and steady-state anisotropies at each temperature and the intrinsic probe limiting anisotropy of DPH [r_0 = 0.4; Kawato et al. (1977) report 0.395; Lakowicz et al. (1979) report 0.390] were used to compute the motional parameters of PHpPC in DPPC LMV.

Fluorescence anisotropy measurements of a 0.1 mM DPPC LMV sample were recorded every 0.2 or 0.5 °C at a scan rate of ±30 °C/h. Details of the method have been described elsewhere (Lentz et al., 1978).

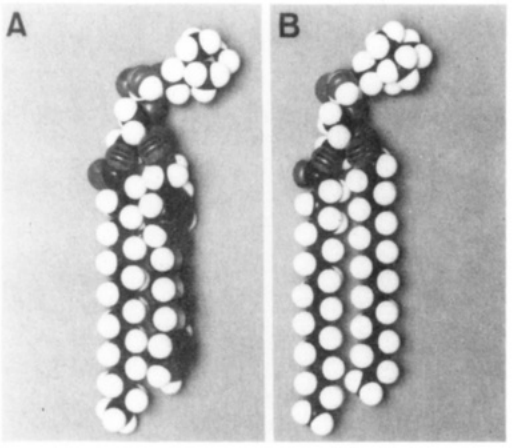

FIGURE 1: Space-filling models of DPHpPC (A) and DPPC (B) molecules as they would be oriented next to each other in the bilayer. Fatty acid chains are in the trans configuration.

Probe Partition Coefficient. The partitioning of DPHpPC was determined in a DMPC/DSPC LMV system with samples made to contain 5, 10, 25, 45, 65, 80, and 95 mol % DMPC. The anisotropy and intensity were measured for each sample at three temperatures. These temperatures (32, 38, and 44 °C) are above the main phase transition temperature of pure DMPC (23.5 °C) and below that of DSPC (54.5 °C). The intensity was corrected at each temperature against a reference standard of POPOP in absolute methanol. Mole fractions of coexisting fluid- and solid-phase lipid in a given sample were determined from the lever rule and reported phase diagrams (Lentz et al., 1976; Luna & McConnell, 1978). The partition coefficient was determined from the anisotropy values and the computed mole fractions of different phases. Anisotropy values were calculated from an assigned partition coefficient and were compared to observed anisotropy data by a χ-square minimization. Equations to calculate the partition coefficient are presented in Lentz et al. (1976).

Calorimetry. A Tronac 750 high-sensitivity, differential scanning calorimeter constructed by Roger Hart (Hart Scientific, Orem, UT) was used to record phospholipid heat capacity while heating and subsequently cooling vesicle samples (0.5–3 mg of lipid in 50 mM KCl). Experiments were performed at a scan rate of ±15 °C/h, and data were collected and analyzed at an interval of approximmtely 0.05 °C.

Results and Discussion

For the majority of experiments, DPHpPC was incorporated into DPPC LMV, since many physical measurements have already been made with this lipid system. A space-filling model of a DPHpPC molecule is shown in Figure 1A next to a fully extended, *all-trans*-DPPC molecule (Figure 1B). One should note that the length of the DPH-containing chain is comparable to that of a 16-carbon chain in the trans configuration. As a result, this molecule should fit well into the bilayer lipid matrix.

Absorption and Emission. The spectral properties of DPHpPC are similar to those of DPH. The excitation spectrum has been reported (Morgan et al., 1982) to have an absorption maximum equivalent to DPH (355 nm). We have determined the extinction coefficient to be 60000 OD M^{-1} cm^{-1} for DPHpPC in $CHCl_3$ as compared to 80000 OD M^{-1} cm^{-1} for DPH in cyclohexane (Berlman, 1971) and $CHCl_3$. Another DPH analogue, TMA-DPH, was also found to have a reduced extinction coefficient (ϵ = 30200 OD M^{-1} cm^{-1} measured in dimethylformamide) while retaining the basic spectral properties of DPH (Prendergast et al., 1981).

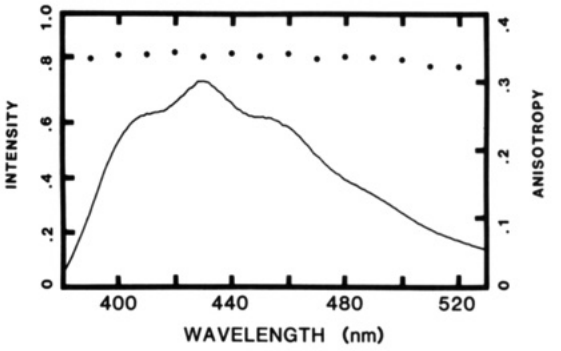

FIGURE 2: Fluorescence emission spectrum of DPHpPC in DPPC LMV. Vesicles containing DPHpPC at a lipid to probe ratio of 400:1 (0.15 mM DPPC) were suspended in 50 mM KCl. The emission spectrum was recorded at 25 °C and corrected for instrument response and sample blanks. This spectrum was nearly identical with one recorded for DPH (data not shown). The closed circles correspond to steady-state fluorescence anisotropy measurements recorded at 10-nm intervals throughout the emission band.

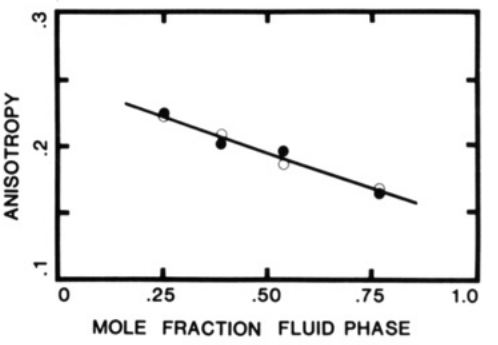

FIGURE 3: Fluorescence anisotropy as a function of mole fraction fluid phase, as determined from the phase diagram for mixed DMPC/DSPC LMV (see Methods). Closed circles represent the observed anisotropy values, while open circles are the calculated anisotropy values obtained with a partition coefficient of $K_{f/s}$ = 3.3. The solid line was determined by a least-squares fit to the calculated points. Data were obtained at 32, 38, and 44 °C in the mixed fluid and solid region of the phase diagram described for mixtures of these two lipids (Lentz et al., 1976; Luna & McConnell, 1978).

Figure 2 shows the corrected emission spectrum of DPHpPC recorded at 25 °C in DPPC LMV at a 400:1 lipid to probe ratio. This spectrum agrees with that of DPHePC (Morgan et al., 1982) and with the spectrum of DPH (Prendergast et al., 1981). Steady-state fluorescence anisotropy measurements were recorded at 25 °C at 10-nm intervals across the emission band. Anisotropy did not vary with emission wavelength as shown by the closed circles in Figure 2. Likewise, the anisotropy was unchanged across the emission band for DPH and TMA-DPH (Prendergast et al., 1981).

Probe Partitioning. Mixed large vesicles (LMV) composed of known amounts of DMPC/DSPC were used to study the partitioning of DPHpPC between gel and liquid-crystalline phases. This lipid mixture was chosen since the phase diagram had been determined (Lentz et al., 1976; Luna & McConnell, 1978) and showed a wide temperature range in which gel and liquid-crystalline states coexisted. In Figure 3, the observed anisotropy (closed circles) is plotted vs. mole fraction of fluid component (as determined from the phase diagrams). The best partition coefficient to fit the data was found to be $K_{f/s}$ = 3.3. Values of the anisotropy calculated from this partition coefficient are also plotted (open circles) and are very close to the observed values. The line drawn through the calculated points were obtained by a least-squares regression. These data indicate a 3:1 preference of DPHpPC for the fluid relative to the gel phase. In contrast, DPH has been shown to have a

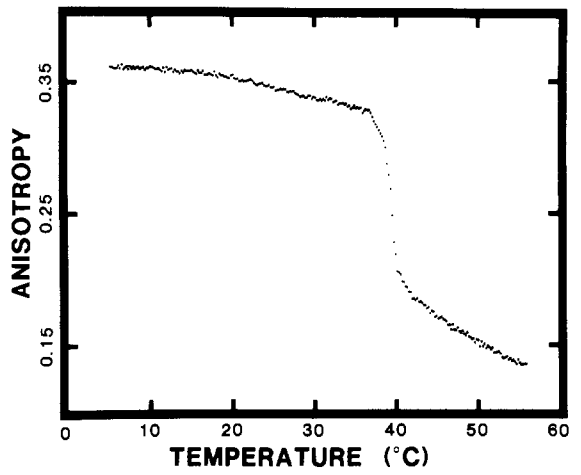

FIGURE 4: Steady-state fluorescence anisotropy of DPHpPC in DPPC LMV as a function of temperature. The cooling scan depicted was recorded at a scan rate of 30 °C/h at 0.2 °C intervals. Vesicles contained 0.25 mol % probe and were examined at a final lipid concentration of 0.1 mM.

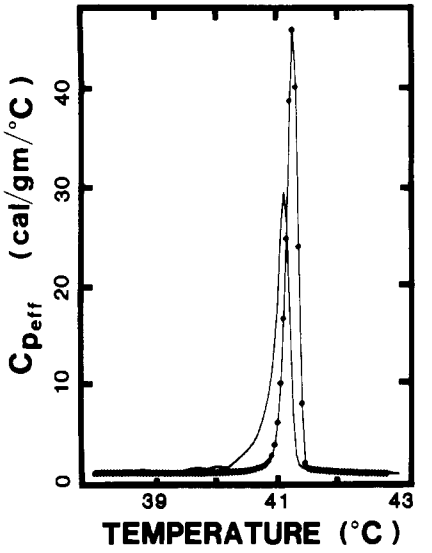

FIGURE 5: Temperature dependence of the molar heat capacity (C_P) of DPPC LMV (1 mg in 1.5 mL of 50 mM KCl) in the absence (diamonds) and presence (solid line) of 2 mol % DPHpPC. Data were obtained at a heating scan rate of 15 °C/h. Cooling scans on the same samples were essentially identical. Similar data were obtained with a sample containing only 0.25 mol % DPHpPC in DPPC.

partition coefficient of roughly 1.0 between gel and fluid phases (Lentz et al., 1976). Another amphipathic DPH-containing probe, TMA-DPH, displayed a similar preference for the fluid phase ($K_{f/s}$ = 3.2) when DMPC was added to DPPC vesicles preincubated with probe (data not shown). The similar partitioning behavior of DPHpPC and TMA-DPH may reflect how these amphipathic analogues are constrained to remain aligned with the lipid acyl chains in the bilayer. In contrast, the nonpreferential partitioning of DPH may result from the freedom of DPH to assume other orientations in less ordered regions near the center of the bilayer (Lentz et al., 1976).

Fluorescence Anisotropy through the Phospholipid Phase Transition. Figure 4 shows changes in the steady-state anisotropy of DPHpPC in DPPC LMV over a broad temperature range. The cooling scan shown here is virtually superimposable with a subsequent heating scan (±30 °C/h). While the general shape of the curve is similar to that obtained with DPH (Lentz et al., 1978), there are two significant differences. First, the anisotropy of DPHpPC fluorescence leveled off at a higher value above the phase transition (e.g., 0.15 for DPHpPC vs. 0.08 for DPH at 50 °C). This plateau indicates that the motion of the DPH moiety is limited at high temperature due to its covalent attachment within a lipid molecule. A similar pattern was seen with TMA-DPH (Prendergast et al., 1981).

The second major difference in the behavior of the fluorescence anisotropy of DPHpPC relative to DPH is in the phase transition temperature reported by the two probes. As previously demonstrated, lipid phase transitions can be conveniently detected by fluorescence depolarization of DPH (Lentz et al., 1976, 1978). The derivative of the anisotropy with respect to temperature (a parameter that contains information comparable to that contained in the derivative of the natural logarithm of the microviscosity with respect to temperature; Lentz et al., 1978) enables one to obtain the peak temperature for the main order to disorder transition. This phase transition temperature was reported by DPHpPC as 39.5 °C for the cooling scan shown in Figure 4. The transition temperature obtained with DPHpPC was 1.1 °C lower than that detected by DPH in heating/cooling scans of DPPC LMV (Lentz et al., 1978). A slightly lower phase transition temperature (39.0 °C) was observed in a scan with DPHePC (from E. W. Thomas), and the breadth of the transition was increased 2.5-fold, consistent with the presence of a small impurity in this probe preparation (see Materials). Only the anisotropy values reported by DPHePC in the region of the phase transition were altered relative to DPHpPC; anisotropy values at the temperature extremes were unchanged.

The difference in the gel/fluid phase partition coefficients of DPH and DPHpPC offers a possible explanation for the different transition temperatures reported by these two probes. Since DPHpPC molecules have a 3:1 preference for fluid-phase regions of the bilayer, they will partition into and preferentially report the occurrence of any fluid domains that form as the phase transition is approached. Work with other fluorescent membrane probes showing unequal partitioning behavior supports the idea that preferential partitioning into fluid- or gel-phase lipid results in the probe reporting a lower or higher phases transition temperature, respectively. For example, Sklar et al. (1979) have reported that *trans*-parinaric acid partitions into solid-phase lipid ($K_{s/f}$ = 5) and detects the DPPC phase transition at 42 °C (1.4 °C higher than reported by DPH). In addition, our laboratory has recently shown that phospholipids containing pyrenyldecanoic acid partition preferentially into fluid-phase regions of membranes ($K_{f/s}$ = 7) and report the phospholipid phase transition in DPPC LMV at a lower temperature (39.0 °C) than DPH fluorescence or calorimetry (Jones & Lentz, 1985).

Another possible explanation for the failure of DPHpPC to accurately report the phase behavior of DPPC LMV is a local perturbation of the DPHpPC environment. Such a perturbation could induce local melting below the bulk phase transition temperature of the overall membrane. In this instance, one might expect these melted local domains to coalesce, resulting in a high local concentration of DPHpPC. Our calorimetric and fluorescence lifetime results (below) will help distinguish between these two possibilities.

Differential Scanning Calorimetry. Heating and cooling calorimetric scans were performed on DPPC LMV containing 2.0 and 0.25 mol % DPHpPC to help determine the cause of the lowered phase transition reported by DPHpPC fluorescence anisotropy measurements. Figure 5 demonstrates the difference in calorimetric scans in the presence and absence of DPHpPC. Relative to pure DPPC LMV, only slight changes (0.1–0.2 °C) in the main peak transition temperatures and essentially no change in transition width at half-height were

Table I: Fluorescence Lifetime Heterogeneity Analysis of DPHpPC and DPHePC[a]

temp (°C)	single lifetimes, τ (ns)	dual lifetimes τ_1 (ns)	dual lifetimes τ_2 (ns)	dual lifetimes f_2	statistical analysis F_{12}	statistical analysis P
		(A) DPHpPC				
8	6.56	7.13	5.30	0.28	0.92	0.60
17	6.61	6.70	0.04	0.01	1.08	0.58
25	7.15	7.50	6.62	0.37	0.64	0.62
31	7.16	8.35	5.06	0.31	2.45	0.51
43	6.99	7.05	7.68	0.06	0.63	0.73
47	6.83	6.85	6.85	0.37	0.64	0.62
52	6.40	7.11	3.23	0.15	0.74	0.68
		(B) DPHePC				
8	6.26	6.59	2.67	0.08	5.99	0.11
17	6.45	6.78	2.75	0.08	4.35	0.17
25	6.62	6.95	2.76	0.07	3.73	0.21
31	6.73	7.07	2.74	0.07	3.52	0.25
43	6.60	6.86	2.63	0.06	2.69	0.32
47	6.48	6.75	2.70	0.06	2.82	0.29
52	6.34	6.61	2.70	0.07	3.59	0.21

[a] τ = lifetime from one-component analysis. τ_1 and τ_2 = lifetimes from two-component analysis. f_2 = fractional fluorescence intensity of component having lifetime τ_2. F_{12} = ratio of reduced χ squares for the one-component relative to the two-component fit (Bevington, 1969). P = probability that a single-exponential decay describes the data.

observed when DPHpPC was present. A low-temperature shoulder that broadened the base of the transition was observed in the presence of DPHpPC (Figure 5, solid line). The broadening occurred only at the low-temperature edge of the transition, consistent with the partitioning of DPHpPC into the fluid phase. Under similar experimental conditions (Lentz et al., 1978), 2 mol % DPH (which does not preferentially partition into gel or fluid lipid; Lentz et al., 1976) in DPPC LMV caused a 0.5 °C lowering of the transition temperature, no change in transiton width, and no broadening at the base of the transition. The small effect of DPH and DPHpPC on the transition peak position and on half-width is consistent with only a minor perturbing effect of these probes on the overall cooperative phase transition. However, the difference in the calorimetric and fluorometric measurements of the phase transition indicates that the fluorescence measurements are more sensitive to the immediate probe environment than to the bulk lipid cooperative phase transition.

In addition to the main heat capacity peak at 41.1 °C, one observes, in Figure 5, a slight elevation in the heat capacity between 39.5 and 40.2 °C. An identical heat capacity elevation was seen with membranes containing 0.25 mol % DPHpPC. This is the same temperature region in which DPHpPC fluorescence anisotropy reported the phase transition (Figure 4). This observation is consistent with the possible existence of locally disrupted gel-phase structure in the presence of DPHpPC. This local perturbation is not extensive or it would be more easily observable by calorimetric measurements.

Fluorescence Lifetime. The fluorescence lifetime of DPHpPC and DPHePC in DPPC LMV was investigated as a function of temperature. Data collected at three modulation frequencies (6, 18, and 30 MHz) were analyzed in terms of one or two lifetime components as described by Barrow & Lentz (1983, 1985). The ratio of reduced χ-square values obtained from our analysis is distributed according to the F distribution (Bevington, 1969). This calculated ratio, F_{12}, is a measure of the improvement that a two-component fit makes relative to a one-component fit. F_{12}, along with the appropriate number of degrees of freedom, can be used to calculate the probability that any improvement in the reduced χ-square value for a two-component relative to a one-component fit might be due to statistical fluctuations in the data (Bevington, 1969). We have chosen a probability of ≥ 0.5 to indicate that a one-component fit best describes the data.

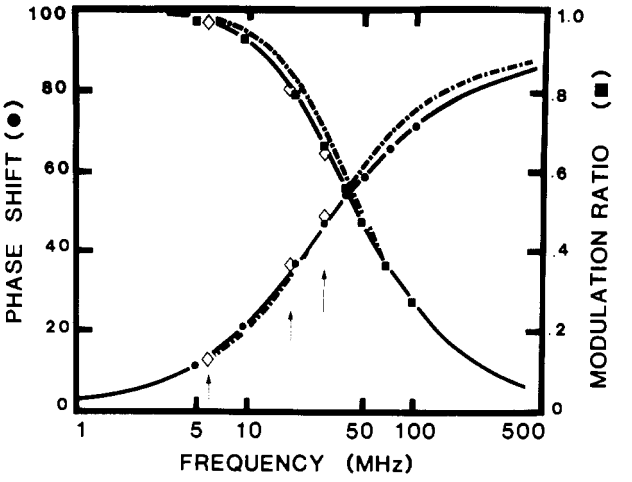

FIGURE 6: Modulation ratio and phase-shift values obtained as a function of frequency with a multifrequency phase fluorometer. Raw data for phase shift (circles) and modulation ratio (squares) are shown and were analyzed with a one-component (dashed line) or two-component (solid line) fit. The two-component analysis fit the data points quite well (reduced χ square = 0.31). Arrows at 6, 18, and 30 MHz point to data (diamonds) obtained with the commercial SLM instrument.

Table I summarizes the lifetime behavior at selected temperatures above and below the DPPC phase transition. Data obtained with DPHpPC were described (with overall 62% probability) by a single-component lifetime throughout the temperature range. In contrast, the lifetime data from DPHePC indicated a more favorable fit by a two-component analysis. A fairly constant low-lifetime component of 2–3 ns accounted for approximately 7% of the total fluorescence intensity from DPHePC. Using the same source of DPHePC, Cranney et al. (1983) reported a major lifetime component of 7.6 ns and a minor component (26% of total fluorescence intensity) of 3.0 ns measured at 25 °C in DPPC vesicles; while Stubbs et al. (1984) reported a major component of 6.02 ns and a minor component (25% of total fluorescence intensity) of 1.53 ns at 37 °C in lipid vesicles derived from sarcoplasmic reticulum. As presented in Table IB, our results for DPHePC are in reasonable agreement with these reports. One should notice that the resolved major lifetime component for the DPHePC (τ_1, Table IB) agrees well with the single lifetime observed for DPHePC (τ, Table IA).

We are fortunate to have had the opportunity to measure the lifetime of a sample containing DPHpPC at a few discrete temperatures with the multifrequency phase fluorometer described by Gratton & Limkeman (1983). The limit of resolution for a 2-ns component in a DPHpPC-containing sample is approximately 3 intensity % with an SLM 4800 phase fluorometer. The multifrequency instrument is capable of resolving two lifetime components beyond these limits. We obtained data at 20, 43, and 51 °C, which were analyzed in terms of one- and two-component fits (Lakowicz et al., 1985). Figure 6 shows the raw data obtained (circles, phase-angle shifts; squares, modulation ratios) as a function of modulation frequency at 51 °C. The dashed line is the one-component fit to the data while the solid line is the two-component fit. The phase shift curves nearly coincide below modulation frequencies of 50 MHz, but it is obvious that the two-component fit best describes the observed data at higher modu-

Table II: Fluorescence Lifetime Heterogeneity Analysis of DPHpPC Derived from Continuous Frequency Data[a]

temp (°C)	single lifetimes, τ (ns)	dual lifetimes τ_1 (ns)	dual lifetimes τ_2 (ns)	dual lifetimes f_2	statistical anal., F_{12}
20	5.76	6.32	1.54	0.05	23
43	5.87	6.42	2.22	0.07	33
51	5.60	6.17	2.05	0.07	87

[a] τ = lifetime from one-component analysis. τ_1 and τ_2 = lifetimes from two-component analysis. f_2 = fractional fluorescence intensity of component having lifetime τ_2. F_{12} = ratio of reduced χ squares for the one-component relative to the two-component fit.

lation frequencies. In Table II, we summarize the analysis of data obtained with the multifrequency instrument. Both above and below the phase transition temperature, DPHpPC exhibited a major lifetime component of 6.3 ns (94 intensity %) and a minor lifetime component of 2 ns (5–7 intensity %). The errors inherent in phase shift and modulation ratio measurements on our SLM 4800 phase fluorometer should allow resolution of a 2-ns component of this magnitude. Therefore, we suspect that our failure to detect a second lifetime component in DPHpPC samples measured on the SLM 4800 partially reflects different experimental conditions required for use of the multifrequency instrument. Two significant differences relate to excitation frequency and light source. First, an excitation wavelength of 325 nm was used for Gratton's multifrequency instrument vs. 366 nm used on our standard SLM instrument. It is possible that the component responsible for the 2-ns decay time has a greater molar absorption at this lower frequency. Second, the fractional intensity of the 2-ns component in DPH-containing samples has been shown to increase in response to light exposure (Parasassi et al., 1984; Barrow & Lentz, 1985) especially for samples containing unsaturated phospholipids (Parasassi et al., 1984). It may be that different sample handling or the more intense laser excitation source used on the multifrequency instrument led to an increase in the contribution of the 2-ns component.

Despite the slight discrepancy between measurements made on the two instruments, our results for DPHpPC, and those of others (Parasassi et al., 1984; Barrow & Lentz, 1985) for DPH, agree that a second, short-lifetime component of fluorescence decay is present in membranes containing some form of DPH and appears to reflect the presence of a photolysis product that exists even in carefully handled samples exposed to minimal light. It will be difficult to detect this component at less than 3 intensity % with an instrument having a limited range of modulation frequencies (e.g., less than 50 MHz; see Figure 6). Resolution is especially difficult when the major lifetime component is less than 8 or 9 ns, as for DPH above the phase transition (Barrow & Lentz, 1985) or DPHpPC above and below the phase transition (Table IA). In a sample exposed extensively to light or containing some unsaturated phospholipid (as for DPHePC), the short-lifetime component should be more easily detected, even on the commercial, three-frequency instrument. Consistent with this idea, note that the major lifetime components observed under three sets of conditions for DPHpPC or DPHePC were the same, independent of the level of 2-ns component present (Table IA, τ; Table IB, τ_1; Table II, τ_1).

An interesting feature of the fluorescence decay properties of DPHpPC is the decrease in lifetime with decreasing temperature below the main phospholipid phase transition of DPPC (Table I). This is curious, since the lifetime would be

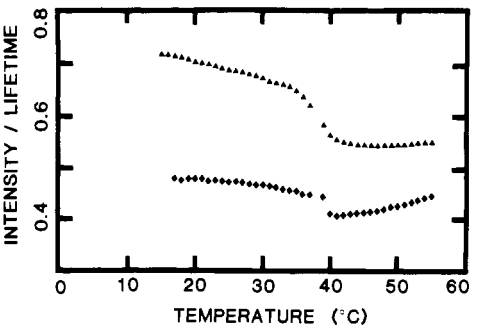

FIGURE 7: Ratio of fluorescence intensity to lifetime as a function of temperature. DPPC LMV were made containing either DPH or DPHpPC. Triangles correspond to data obtained with DPHpPC-containing vesicles, while diamonds represent the DPH-containing sample.

expected to increase in a more restricted environment. A similar effect was seen with DPH but could be explained by a significant increase in the contribution of the low-lifetime component at low temperature (Barrow & Lentz, 1985). This explanation does not appear applicable to the behavior of DPHpPC.

Figure 7 shows the temperature dependence for the ratio of intensity to average lifietime for both DPH (diamonds) and DPHpPC (triangles) in DPPC LMV. The relative intensity measurements for the two samples were normalized such that observed differences in the intensity/lifetime ratio reflect absolute differences in lifetime. For purely dynamic quenching, this ratio should remain constant with temperature. A change at the main lipid phase transition can be observed for both probes. However, the change is much greater for DPHpPC than for DPH. For DPHpPC, the substantial increase in the intensity/lifetime ratio below the phospholipid phase transition temperature derives from the unexpected decrease in average fluorescence lifetime at low temperatures (see Table I). This decreasing lifetime was not accompanied by a proportional drop in fluorescence intensity (Figure 7) and therefore cannot reflect thermal quenching. Both DPH (Barrow & Lentz, 1985) and DPHpPC (R. A. Parente and B. R. Lentz, unpublished) display dramatic drops in lifetime without comparable changes in fluorescence intensity when present at high concentration in the bilayer (i.e., $\geq$1 mol %). Therefore, the decline in DPHpPC lifetime at low temperature is consistent with the existence of probe-enriched regions in the gel phase.

Motional Parameters. We have used differential polarized phase shift measurements to characterize the ability of the DPHpPC molecule to wobble or rotate in a bilayer environment and have analyzed these measurements in terms of a simple treatment of restricted probe motion (Lakowicz et al., 1979). Differential tangent (tan Δ) measurements were recorded over the temperature range from 10 to 58 °C at modulation frequencies of 18 and 30 MHz. The temperature profile is given in Figure 8A, where open squares represent data recorded at 30 MHz and closed triangles data obtained at 18 MHz. In the low-temperature region, data from both 18 and 30 MHz were identical. The solid lines are quadratic fits to the data in regions above and below the phase transition. Low values for tan Δ were observed below the main lipid phase transition and increased sharply as the melting temperature was approached. The tan Δ function would be expected to be zero if the fluorophore were fixed (or if rotations occurred on a time scale much longer than the fluorescence lifetime) (Lakowicz et al., 1979). It is clear that the probe is quite rigidly fixed below the phase transition temperature but ob-

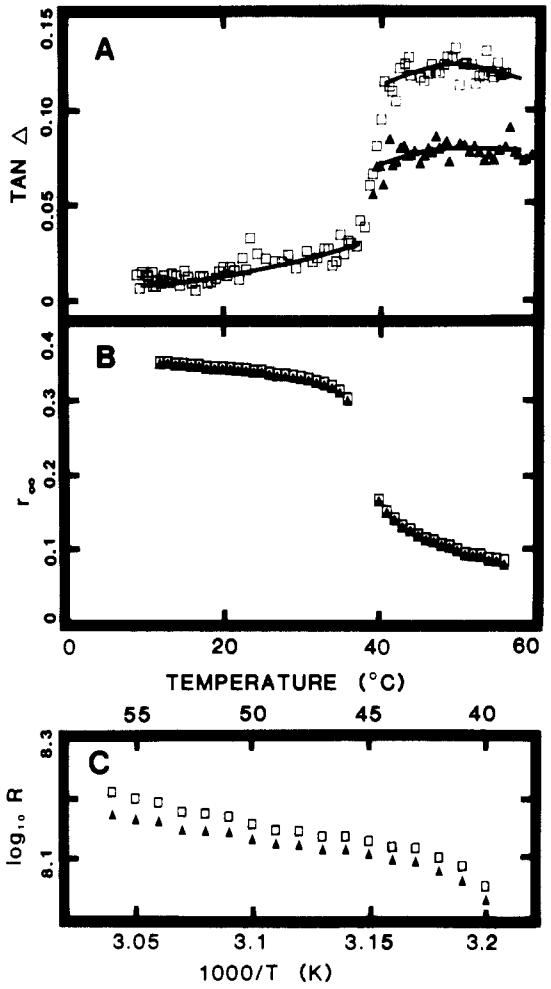

FIGURE 8: Temperature dependence of differential phase fluorescence measurements and derived rotational properties of DPHpPC in 0.1 mM DPPC LMV. Data were recorded at both 18- (closed triangles) and 30-MHz (open squares) modulation frequencies. (A) Differential phase fluorescence measurements made at 18 and 30 MHz and recorded as the differential tangent (tan Δ; Lakowicz et al., 1979). Solid lines illustrate quadratic fits to the raw data. Data obtained at 18 and 30 MHz were superimposable at low temperatures. (B) Temperature dependence of limiting fluorescence anisotropy calculated from the fitted data shown in (A). (C) Temperature dependence of rotational rate obtained (Lakowicz et al., 1979) from the fitted values of differential tangent (A), the measured fluorescence lifetimes (Table I and other data not shown), and anisotropies (Figure 4).

viously gains motional freedom upon passing through the lipid phase transition.

Figure 8B shows the temperature dependence of DPHpPC limiting anisotropy (r_∞) calculated (see Methods) from the quadratic fits to the tan Δ data in Figure 8A. A value of roughly 0.4 would be expected for a completely immobile molecule. It is evident that DPHpPC is in a highly hindered environment at temperatures below the phase transition. Above the phase transition, the extent of probe motion increased as evidenced by the decrease in r_∞. When compared to DPH above the phase transition (Lakowicz et al., 1979), DPHpPC rotational motion was more restricted (e.g., r_∞ was 0.04 for DPH vs. 0.08 for DPHpPC in DPPC vesicles measured at 30 MHz and 55 °C). Using the free rotation in a cone model, Jähnig (1979) has shown that r_∞ is related to the probe orientational order parameter (S_v) by $r_\infty = (2/5)S_v^2$. Our measurements of r_∞ (Figure 8B) yield a value of 0.50 for the probe orientational order parameter at 50 °C. This corresponds to the molecular order parameter obtained by deuterium nuclear magnetic resonance of DPPC deuterated above carbon number 4 of its acyl chains (Seelig & Seelig, 1978). Data for TMA-DPH under similar conditions (Prendergast et al., 1981) yield an even larger value (0.57) for the probe orientational order parameter. It is evident from Figure 1 that the DPH moiety of DPHpPC is located much further down in the hydrocarbon region of the bilayer than carbon number 4. However, the rigid DPH moiety is free to move in the bilayer only to the extent that C–C rotations can occur in the carboxyethyl moiety that attaches DPH to the phospholipid glycerol backbone. It appears that the rotational freedom experienced by the DPH portion of DPHpPC is determined by molecular order in the uppermost portions of the bilayer. This is likely to be the case for any phospholipid-like amphipathic probe containing a lengthy, rigid, hydrophobic fluorophore.

Rotational rate (R) of the DPH portion of DPHpPC within its restricted cone is presented in Figure 8C at temperatures above the phase transition. The fitted values of the differential tangent (from Figure 8A), measured fluorescence lifetimes (from Table I and other data not shown), and anisotropies (from Figure 4) were used to calculate R (see Methods). The rotational rates of DPH in DPPC LMV (Lakowicz et al., 1979) and of DPHpPC (Figure 8C) increased with increasing temperature above the phase transition. Below the phase transition, essentially no rotation was measurable for DPHpPC. Even data collected on the multifrequency instrument of E. Gratton could not be resolved to give meaningful estimates of rotational rate below the transition temperature. Others (Lakowicz et al., 1979; Kawato et al., 1977) have also failed to obtain accurate estimations of R for DPH below the phase transition temperature. We conclude that the angle of rotation for the DPH moiety of DPHpPC is very close to 0° in solid-phase bilayers, making rotations of too small an amplitude to allow accurate measurement of the rotational rate.

Conclusions

The following properties of DPHpPC have been presented and discussed. Unless specifically cited, these properties are probably applicable to DPHePC. (1) DPHpPC shows a 3-fold preference to partition into fluid-phase relative to solid-phase regions of mixed-lipid bilayers. (2) The DPH moiety of DPHpPC is oriented with the bilayer acyl chains at all temperatures and demonstrates fairly restricted motions, reflecting molecular order near the glycerol–acyl chain linkage. (3) DPHpPC and DEHePC exhibit a double fluorescence decay in a phospholipid bilayer with a minor 2-ns component, probably the result of a photolysis product. This component is difficult to detect in saturated lipid samples carefully protected from light (DPHpPC). (4) While DPHpPC has a negligible perturbing effect on the cooperative phase behavior of membranes, its fluorescence anisotropy reports an abnormally low phase transition temperature. (5) Below the phase transition, DPHpPC appears to perturb its local environment and may segregate into probe-enriched domains that melt at somewhat lower temperatures than the bulk lipid. Knowledge of these properties should help to make DPHpPC an extremely useful probe of membrane structure.

Acknowledgments

We thank Dennis R. Alford for critical reading of the manuscript and Dr. Emrys Thomas of the University of Salford (U.K.) for supplying initial samples of DPHePC and its precursor, carboxyethyl-DPH. We are also grateful to Dr. Walter Shaw for his cooperation in the timely and careful synthesis of DPHpPC. Finally, we thank Dr. Enrico Gratton

for generously offering the use of his multifrequency phase fluorometer.

Registry No. DPH_pPC, 98014-38-1.

REFERENCES

Barrow, D. A., & Lentz, B. R. (1983) *J. Biochem. Biophys. Methods 7*, 217–234.
Barrow, D. A., & Lentz, B. R. (1985) *Biophys. J. 48*, 221–234.
Berlman, I. B. (1971) *Handbook of Fluorescence Spectra of Aromatic Molecules*, 2nd ed., p 322, Academic Press, New York.
Bevington, P. R. (1969) *Data Reduction and Error Analysis for the Physical Sciences*, Chapter 10, McGraw-Hill, New York.
Cranney, M., Cundall, R. B., Jones, G. R., Richards, J. T., & Thomas, E. W. (1983) *Biochim. Biophys. Acta 735*, 418–425.
Gratton, E., & Limkeman, M. (1983) *Biophys. J. 44*, 315–324.
Jones, M. E., & Lentz, B. R. (1985) *Biochemistry* (submitted for publication).
Kawato, S., Kinosita, K., Jr., & Ikegami, A. (1977) *Biochemistry 16*, 2319–2324.
Lakowicz, J. R., Prendergast, F. G., & Hogen, D. (1979) *Biochemistry 18*, 508–519.
Lakowicz, J. R., Cherek, H., Maliwal, B. P., & Gratton, E. (1985) *Biochemistry 24*, 376–383.
Lentz, B. R., Barenholz, Y., & Thompson, T. E. (1976) *Biochemistry 15*, 4529–4537.
Lentz, B. R., Freire, E., & Biltonen, R. L. (1978) *Biochemistry 17*, 4475–4480.
Luna, E. J., & McConnell, H. M. (1978) *Biochim. Biophys. Acta 509*, 462–473.
Morgan, C. G., Thomas, E. W., Moras, T. S., & Yianni, Y. P. (1982) *Biochim. Biophys. Acta 692*, 196–201.
Parasassi, T., Conti, F., Glaser, M., & Gratton, E. (1984) *J. Biol. Chem. 259*, 14011–14017.
Prendergast, F. G., Haugland, R., & Callahan, P. J. (1981) *Biochemistry 20*, 7333–7338.
Seelig, A., & Seelig, J. (1978) *Hoppe Seyler's Z. Physiol. Chem. 359*, 1747–1756.
Shinitzky, M., & Barenholz, Y. (1978) *Biochim. Biophys. Acta 515*, 367–394.
Sklar, L. A., Miljanich, G. P., & Dratz, E. A. (1979) *Biochemistry 18*, 1707–1716.
Spencer, R. D., & Weber, G. (1969) *Ann. N.Y. Acad. Sci. 158*, 361–376.
Stubbs, C. D., Kinosita, K., Jr., Munkonge, F., Quinn, P. J., & Ikegami, A. (1984) *Biochim. Biophys. Acta 775*, 374–380.

Ia-Associated Invariant Chain Is Fatty Acylated before Addition of Sialic Acid†

Norbert Koch* and Günter J. Hämmerling
Institute of Immunology and Genetics, German Cancer Research Center, D-69 Heidelberg, Federal Republic of Germany
Received February 13, 1985

ABSTRACT: The murine invariant chain (Ii) was found to incorporate radioactive palmitic acid. This binding of fatty acid inhibits the formation of interchain S–S bonds, probably because the cysteine residue in the transmembrane region of the Ii chain is palmitylated. The inhibition of fatty acylation by cerulenin blocks further posttranslational maturation of the invariant chain as shown by two-dimensional gel electrophoresis of Ii immunoprecipitates. In particular, the addition of sialic acid residues is blocked. Thus, it appears that fatty acylation is essential for carbohydrate processing of the Ii chain.

The immune response to soluble antigens is regulated by Ia antigens encoded by the I region of the major histocompatibility complex on chromosome 17 of the mouse. Ample evidence suggests that T lymphocytes can recognize antigens only in association with Ia antigens on the surface of antigen-presenting cells [for a review, see Unanue (1981)]. However, little is known about the molecular mechanism of antigen presentation.

Ia antigens consist of polymorphic integral membrane glycoproteins which form two heterodimers, $A_\alpha A_\beta$ and $E_\alpha E_\beta$. These dimers are expressed on the surface of macrophages, blymphocytes, and several other cell types (Hämmerling, 1976). Early after their synthesis Ia antigens are linked to a nonpolymorphic polypeptide of M_r 31 000, designated the invariant (Ii) chain (Jones et al., 1978). This Ia–Ii complex is transient and is dissociated during transport of Ia antigens to the plasma membrane. The cytoplasmic site of this separation of Ia and Ii is not known.

Previously we and others have observed that there is more than one species of invariant chains associated with murine Ia antigens. Of this family of invariant polypeptides the Ii chain is the most abundant (Koch & Hämmerling, 1982; Zecher et al., 1984). At least two of the polypeptides, the Ii chain and a polypeptide of M_r at 41 000, are structurally closely related and are encoded by the same gene (Yamamoto et al., 1985).

Analogues of the mouse invariant chain have been observed in human (Charron & McDevitt, 1979), in rat (Frelinger et al., 1979), in hamster (Sung et al., 1982) and in guinea pig (Quill & Schwartz, 1983) cells. The function of the Ii chain is not known. However, the fact that in all species investigated so far invariant chains are associated with Ia antigens suggests that invariant chains are involved in expression or assembly of Ia, or in its biological function.

Human (Strubin et al., 1984; Claesson et al., 1983) and mouse (Singer et al., 1984) invariant chain cDNA sequences are known. The deduced amino acid sequences exhibit a homology of 73% [reviewed in Long (1985)]. This highly conserved primary structure explains many features common

† This work was supported by Grant Ko 810/2-1 by the Deutsche Forschungsgemeinschaft.

0006-2960/85/0424-6185$01.50/0